

Three Autocatalysts and Self-Inhibition in a Single Reaction: A Detailed Mechanism of the Chlorite–Tetrathionate Reaction

Attila K. Horváth,^{*,†} István Nagypál,[†] and Irving R. Epstein^{*,‡}

Department of Physical Chemistry, University of Szeged, P.O.Box 105, Szeged H-6701, Hungary,
and Department of Chemistry and Volen Center for Complex Systems, MS 015, Brandeis
University, Waltham, Massachusetts 02454-9110

Received July 18, 2006

The chlorite–tetrathionate reaction has been studied spectrophotometrically in the pH range of 4.65–5.35 at $T = 25.0 \pm 0.2$ °C with an ionic strength of 0.5 M, adjusted with sodium acetate as a buffer component. The reaction is unique in that it demonstrates autocatalysis with respect to the hydrogen and chloride ion products and the key intermediate, HOCl. The thermodynamically most-favorable stoichiometry, $2\text{S}_4\text{O}_6^{2-} + 7\text{ClO}_2^- + 6\text{H}_2\text{O} \rightarrow 8\text{SO}_4^{2-} + 7\text{Cl}^- + 12\text{H}^+$, is not found. Under our experimental conditions, chlorine dioxide, the chlorate ion, or both are detected in appreciable amounts among the products. Initial rate studies reveal that the formation of chlorine dioxide varies in an unusual way, with the chlorite ion acting as a self-inhibitor. The reaction is supercatalytic (i.e., second order with respect to autocatalyst H^+). The autocatalytic behavior with respect to Cl^- comes from chloride catalysis of the chlorite–hypochlorous acid and hypochlorous acid–tetrathionate subsystems. A detailed kinetic study and a model that explains this unusual kinetic behavior are presented.

Introduction

The chlorite–thiosulfate reaction displays a remarkable range of “exotic” kinetic phenomena, including complex periodic and aperiodic oscillation^{1,2} and chaos³ in a flow reactor and extreme sensitivity to stirring rate effects and fluctuations⁴ under batch conditions. To date, no attempt has been made to unravel the kinetics and mechanism of the full reaction system because of its complexity. Three long-lived intermediates and end-products, tetrathionate, hypochlorous acid, and chlorine dioxide, have been shown to react further not only with the reactants but also with each other, making the mechanism particularly complicated. During the past two decades, the kinetics and mechanisms of several subsystems of the parent reaction, including hypochlorous acid–chlorite,⁵ thiosulfate–chlorine dioxide,⁶ tetrathionate–hypochlorous acid,⁷ tetrathionate–chlorine dioxide,⁸ sulfite–

chlorine dioxide⁹ and the decomposition of chlorous acid,¹⁰ have been elucidated. Recently, a five-step model was proposed¹¹ for interpreting the unusual kinetic behavior of the chlorite–tetrathionate reaction, in which HSO_3^- plays a crucial role in regulating the concentration of the autocatalyst HOCl. It has also been shown¹² that the reaction proceeds via parallel pathways: a direct reaction and an indirect HOCl-catalyzed path. This simplified model, however, accurately describes only the early stages of the reaction but fails to predict the behavior of the system on a longer time scale and does not explain the chloride catalysis. Here, we present a more detailed kinetic study and propose an extended kinetic model that is able to explain the formation of chlorine dioxide up to 50–100% of the total conversion.

Experimental Section

Materials. Commercially available NaClO_2 (Sigma-Aldrich) was purified as described previously.⁵ The purity of NaClO_2 was

* To whom correspondence should be addressed. E-mail: epstein@brandeis.edu (I.R.E.); horvath@chem.u-szeged.hu (A.K.H.)

[†] University of Szeged.

[‡] Brandeis University.

(1) Orbán, M.; De Kepper, P.; Epstein, I. R. *J. Phys. Chem.* **1982**, *86*, 431.

(2) Orbán, M.; Epstein, I. R. *J. Phys. Chem.* **1982**, *86*, 3907.

(3) Maselko, J.; Epstein, I. R. *J. Chem. Phys.* **1984**, *80*, 3175.

(4) Nagypál, I.; Epstein, I. R. *J. Phys. Chem.* **1986**, *90*, 6285.

(5) Peintler, G.; Nagypál, I.; Epstein, I. R. *J. Phys. Chem.* **1990**, *94*, 2954.

(6) Horváth, A. K.; Nagypál, I. *J. Phys. Chem. A* **1998**, *102*, 7267.

(7) Horváth, A. K.; Nagypál, I. *Int. J. Chem. Kinet.* **2000**, *32*, 395.

(8) Horváth, A. K.; Nagypál, I.; Epstein, I. R. *J. Phys. Chem. A* **2003**, *107*, 10063.

(9) Horváth, A. K.; Nagypál, I. *J. Phys. Chem. A* **2006**, *110*, 4753.

(10) Horváth, A. K.; Nagypál, I.; Peintler, G.; Epstein, I. R.; Kustin, K. *J. Phys. Chem. A* **2003**, *107*, 6966.

(11) Horváth, A. K.; Nagypál, I.; Peintler, G.; Epstein, I. R. *J. Am. Chem. Soc.* **2004**, *126*, 6246.

Table 1. Initial Reactant Concentrations^a

no.	[ClO ₂ ⁻] ₀ (mM)	[S ₄ O ₆ ²⁻] ₀ (mM)	[Cl ⁻] ₀ (mM)
1–16	0.5, 0.7, 1.0, 1.4	0.5	0
17–32	2.0, 3.0, 5.0, 7.0	0.5	0
33–44	10.0, 14.0, 17.0	0.5	0
45–56	20.0, 25.0, 30.0	0.5	0
57–72	5.0	0.1, 0.14, 0.2, 0.3	0
73–88	5.0	0.5, 0.7, 0.8, 0.9	0
89–100	5.0	1.0, 1.2, 1.4	0
101–112	5.0	2.0, 3.0, 5.0	0
113–132	5.0	0.3	0, 1.0, 3.0, 6.0, 10
133–152	5.0	0.14	0, 1.0, 3.0, 6.0, 10

^a Each composition was studied at 4 different pHs.

checked by standard iodometric titration and found to be better than 99.5%. No chloride impurities could be detected in the purified NaClO₂. All other chemicals (K₂S₄O₆, acetic acid, sodium acetate, and sodium chloride) were of the highest purity available (Sigma-Aldrich and Fluka) and were used without further purification.

Acetic acid–acetate buffer was used to maintain the pH between 4.65 and 5.35. The ionic strength was adjusted to 0.5 M with sodium acetate as a buffer component, and the desired amount of acetic acid was added to adjust the pH, taking the pK_a of acetic acid as 4.55. Table 1 shows the initial composition of the solutions studied in the kinetic runs. Each composition was studied at 4 different pHs: 4.65, 4.85, 5.07, and 5.35.

Methods. The kinetic measurements were carried out in a standard 1 cm quartz cuvette equipped with a Teflon cap and a magnetic stirrer. The cuvette was carefully sealed with Parafilm at the Teflon cap to minimize the loss of chlorine dioxide. The reaction was followed at 400 nm with a Zeiss Specord S10 diode array spectrophotometer, excluding ultraviolet light to avoid the photochemical decomposition of tetrathionate ion.¹³ This wavelength was chosen instead of the absorption maximum of ClO₂ at 359 nm to minimize any contribution from the chlorite ion at higher chlorite concentrations.

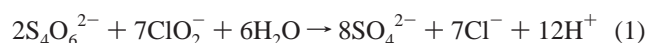
Data Treatment. Only experimental data with values up to 1.0 absorbance unit were used for evaluation of the kinetic runs because the relative error of the absorbance measurements is not acceptable at higher absorbances. Since each kinetic curve contained 250–300 data points, the number of points in each run was reduced to 70 to avoid unnecessary and time-consuming calculations. The reduction was achieved by normalizing the data to fit in a square of unit size and then deleting points to increase the shortest distance between pairs of points at each step until the desired final number of points was reached. The final data are then renormalized to the original scale. This process results in kinetic curves with smooth distributions of points that represent all portions of the curve accurately.¹⁴ In the visible range, the only absorbing species found was chlorine dioxide, so the evaluation procedures were executed at only a single wavelength, 400 nm.

The experimental curves were analyzed with the program package ZiTa.¹⁵ Altogether, 10 640 experimental points from 152 absorbance–time series were used for simultaneous fitting. The sum of squares of the deviations between the measured and calculated absorbances was selected as the parameter to be minimized. Since,

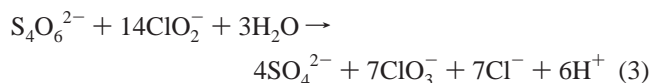
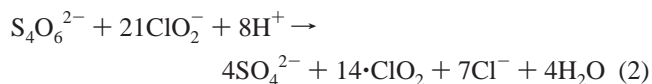
in several kinetic runs, the final absorbance of chlorine dioxide did not reach 0.1 absorbance units, relative fits of the kinetic curves were also conducted (i.e., the deviation between the measured and calculated data was normalized to the largest absorbance change in the given experiment and the sum of squares of these was then minimized). The final kinetic parameters of the proposed model are taken as averages of values from the absolute and relative fits. Our quantitative criterion for an acceptable fit was that the average deviation for the absolute fit approach 0.004 absorbance unit, which is close to the uncertainty of the spectrophotometer. In addition, a satisfactory mechanism was required to qualitatively reproduce all the important characteristics of the measured data such as dependences on initial concentrations and pH.

Results

Stoichiometric Considerations. Several analytical methods have confirmed that the sulfate ion is the only sulfur-containing product after the reaction is complete. However, the thermodynamically most favorable stoichiometry



is never found under our experimental conditions, since chlorine dioxide is almost immediately detected after starting the reaction, even in high excess of tetrathionate. In addition to chlorine dioxide, the chlorate ion is also present among the end-products. As we shall see later, in principle there are two other limiting stoichiometries



but neither of these can be reached experimentally. The complexity of the stoichiometry of the overall reaction reflects that of the subsystems, such as hypochlorous acid–chlorite, sulfite–chlorite, and chlorine dioxide–tetrathionate.

Initial Rate Studies. We have demonstrated earlier¹¹ that the formal kinetic orders of the reactants vary considerably with the initial reactant concentrations. We analyzed the dependence of the stabilized rate (i.e., the rate during the period of constant $\cdot ClO_2$ production), rather than the initial rates. The use of the stabilized rate was suggested by the existence of two qualitatively different types of behavior in the early phase of the kinetic curves. The first type, illustrated by the upper curve in Figure 1, starts with a slow rise in absorbance followed by a faster, nearly linear increase, while the other, seen in the lower curve in Figure 1, begins with a sudden rise in absorbance followed by a slower, linear increase. The linear regime lasts at least several hundred seconds in each kinetic curve and can thus be used to characterize the stabilized rate. The duration of this interval depends strongly on the initial concentrations of the reactants.

The measured stabilized rate shows a maximum as a function of the initial chlorite concentration, as seen in Figure 2. At low [ClO₂⁻]₀, the formal kinetic order of chlorite is between 1 and 2 (the relationship is almost linear), but at

(12) Horváth, A. K. *J. Phys. Chem. A* **2005**, *109*, 5124.

(13) Horváth, A. K.; Nagypál, I.; Epstein, I. R. *J. Am. Chem. Soc.* **2002**, *124*, 10956.

(14) Peintler, G. Manuscript in preparation.

(15) Peintler, G. *ZiTa, A Comprehensive Program Package for Fitting Parameters of Chemical Reaction Mechanisms*, version 5.0; Attila József University: Szeged, Hungary, 1989–1998. This package can be downloaded from the following website: <http://www.staff.u-szeged.hu/~peintler/enindex.htm>.

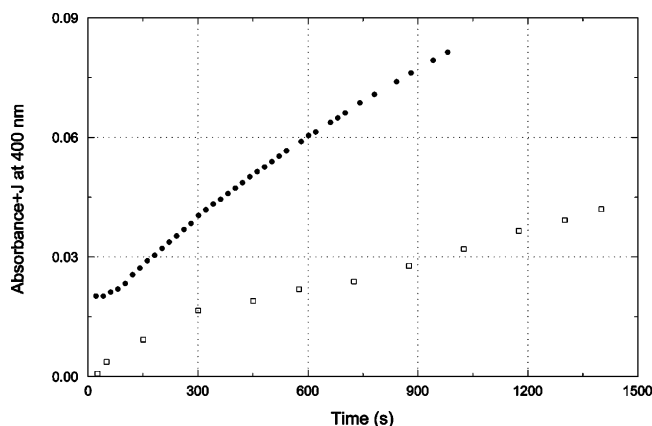


Figure 1. Measured early phase kinetic curves. Initial conditions: $[\text{ClO}_2^-]_0 = 3.0 \text{ mM}$, $\text{pH} = 4.65$, $[\text{S}_4\text{O}_6^{2-}]_0 = 0.5 \text{ mM}$ (●); $\text{pH} = 4.85$, $[\text{ClO}_2^-]_0 = 30.0 \text{ mM}$, $[\text{S}_4\text{O}_6^{2-}]_0 = 0.5 \text{ mM}$ (□). The upper curve (●) is shifted by $J = 0.02$ along the y axis to make the trends clearer. The absorbing species is chlorine dioxide.

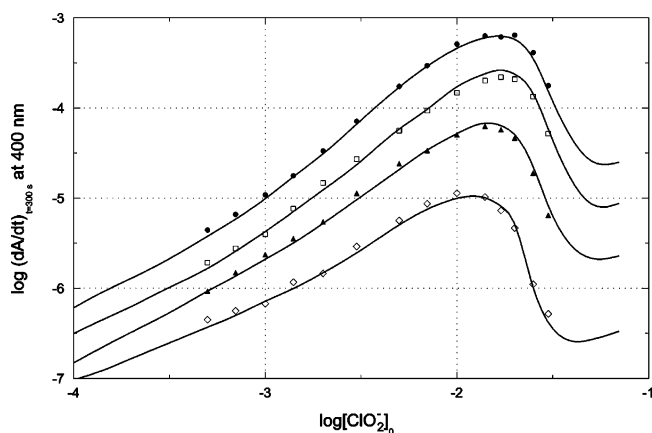


Figure 2. Measured (symbols) and calculated (solid lines) stabilized rates as a function of chlorite concentration at $[\text{S}_4\text{O}_6^{2-}]_0 = 0.50 \text{ mM}$. $\text{pH} = 4.65$ (●), 4.85 (□), 5.07 (▲), and 5.35 (◇). $[\text{Cl}^-]_0 = 0 \text{ M}$.

high chlorite concentration, the rate of formation of chlorine dioxide starts to decrease, implying that chlorite has an inhibitory effect. As shown previously,¹¹ this behavior results from a switch from the fast HOCl-catalyzed reaction to the slow direct reaction. The stabilized rates calculated from the proposed model (see below) show similar trends and also suggest that at higher chlorite concentration ($>0.1 \text{ M}$) the stabilized rate starts to increase again. This complex behavior was pointed out earlier¹¹ and is explained by the increasing importance of the slow direct reaction, which is first order with respect to chlorite.

As shown in Figure 3, the measured stabilized rate increases monotonically with the initial tetrathionate concentration. The formal kinetic order of tetrathionate ion varies between 0 and 1 and decreases with acidity. Under the experimental conditions employed here, we do not observe the unusual high formal kinetic order of tetrathionate because the excess of chlorite is not sufficient to suppress the HOCl-catalyzed pathway. In our previous study,¹¹ more than a 50-fold excess of chlorite was employed. When we explored the behavior of the extended kinetic model at lower initial tetrathionate concentrations corresponding to larger excess of $[\text{ClO}_2^-]_0$, we found, as observed earlier,¹¹ that the formal kinetic order of tetrathionate varies sigmoidally, resulting

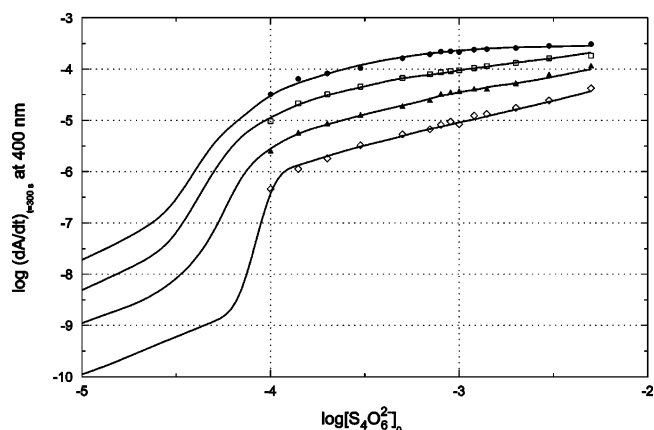


Figure 3. Measured (symbols) and calculated (solid lines) stabilized rates as a function of tetrathionate concentration at $[\text{ClO}_2^-]_0 = 5.0 \text{ mM}$. $\text{pH} = 4.65$ (●), 4.85 (□), 5.07 (▲), and 5.35 (◇). $[\text{Cl}^-]_0 = 0 \text{ M}$.

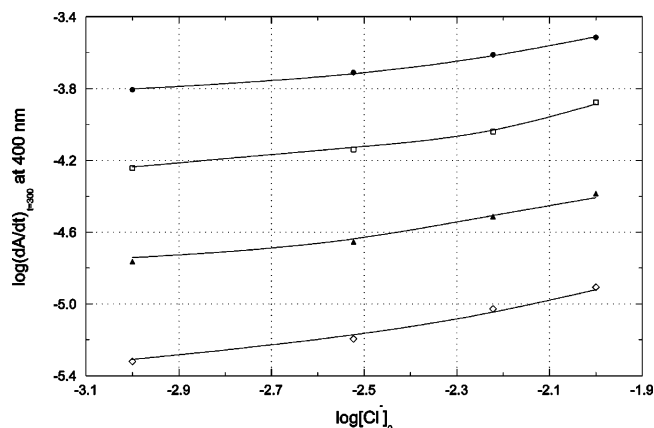


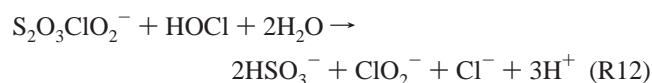
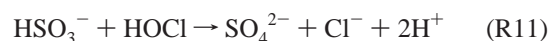
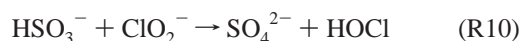
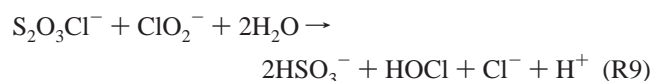
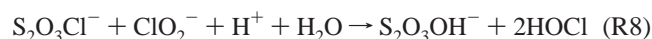
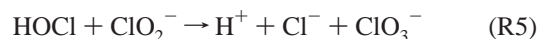
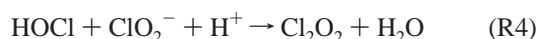
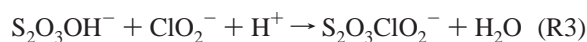
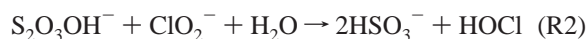
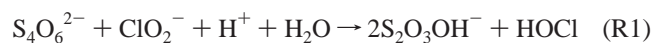
Figure 4. Measured (symbols) and calculated (solid lines) stabilized rates as a function of chloride concentration at $[\text{ClO}_2^-]_0 = 5.0 \text{ mM}$, $[\text{S}_4\text{O}_6^{2-}]_0 = 0.3 \text{ mM}$. $\text{pH} = 4.65$ (●), 4.85 (□), 5.07 (▲), and 5.35 (◇).

in a high formal kinetic order of tetrathionate. This behavior also arises from the switch from the slow direct reaction to the HOCl-catalyzed pathway. The experiments in which $[\text{S}_4\text{O}_6^{2-}]_0$ was varied were not extended to lower tetrathionate concentrations, where only the slow direct reaction governs the formation of chlorine dioxide, because the reaction would have become painfully slow, as seen in Figure 3. One may ask whether our data provide sufficient information about the direct reaction. This information can be obtained from those experiments in which more than a 40-fold molar excess of chlorite is present (experiments 45–56 in Table 1), since the inhibitory effect of chlorite then suppresses the HOCl-catalyzed pathway almost completely.

An early preliminary study of this reaction⁴ has suggested that the product chloride ion also increases the rate of reaction (i.e., that the reaction is autocatalytic not only in H^+ but also in Cl^-). Figure 4 clearly demonstrates this effect, yielding a rough formal kinetic order of 0.3 for chloride. This fractional order and the increase in the formal kinetic order of chloride as a function of $[\text{Cl}^-]_0$ suggest that the chloride ion plays a complex role through its effect on the various subsystems of the parent reaction.

Proposed Kinetic Model. As a starting point to develop a kinetic model that describes the formation of chlorine dioxide over the time course of the reaction, we took the

eight-step mechanism¹² for the initial phase of the reaction, from which the reduced five-step model was derived. Since tetrathionate can also be oxidized by chlorine dioxide under our experimental conditions, we adopted a previously proposed 14-step mechanism for the chlorine dioxide–tetrathionate reaction,⁸ which we refer to as the CDT mechanism, keeping all kinetic parameters unchanged. We then considered all additional mono- and bimolecular reactions of the species in the eight-step model and the CDT mechanism, as well as their H^+ -, OH^- - and Cl^- -catalyzed pathways, a total of more than 600 steps, in our analysis. Lengthy and time-consuming but straightforward systematic reduction of this initial model led to the following set of essential steps:



The corresponding rate equations and the suggested values of the parameters are summarized in Table 2.

Discussion

It is well-established that the rate of initiation of the reaction, step R1, depends on $[\text{H}^+]^2$ (i.e., the reaction is supercatalytic, that is, autocatalytic with an order greater than one, with respect to H^+). This feature of the reaction has been extensively exploited to study the evolution of spatiotemporal structures both experimentally and theoretically.^{16–19} Our suggested rate constant is in reasonable

Table 2. Rate Equations and Rate Coefficients Obtained from the Fitting Procedure^a

	rate equation	suggested params
R1	$k_1[\text{S}_4\text{O}_6^{2-}][\text{ClO}_2^-][\text{H}^+]^2$	$(2.08 \pm 0.16) \times 10^5 \text{ M}^{-3} \text{ s}^{-1}$
R2	$k_2[\text{S}_2\text{O}_3\text{OH}^-][\text{ClO}_2^-]$	$\geq 10 \text{ M}^{-1} \text{ s}^{-1}$
R3	$k_3[\text{S}_2\text{O}_3\text{OH}^-][\text{ClO}_2^-]$	$k_3/k_2 = 0.59 \pm 0.10$
R4	$(k_4 + k'_4[\text{Cl}^-])[\text{HOCl}][\text{ClO}_2^-][\text{H}^+]$	$k_4 = 1.06 \times 10^6 \text{ M}^{-2} \text{ s}^{-1}$ $k'_4 = (5.03 \pm 0.13) \times 10^8 \text{ M}^{-3} \text{ s}^{-1}$
R5	$k_5[\text{HOCl}][\text{ClO}_2^-]$	$5.31 \pm 0.22 \text{ M}^{-1} \text{ s}^{-1}$
R6	$(k_6[\text{H}^+] + k'_6[\text{Cl}^-])[\text{Cl}_2\text{O}_2][\text{ClO}_2^-]$	$k_6 = (1.85 \pm 0.62) \times 10^6 \text{ M}^{-2} \text{ s}^{-1}$ $k'_6 = (4.80 \pm 0.78) \times 10^4 \text{ M}^{-2} \text{ s}^{-1}$
R7	$(k_7 + k'_7[\text{Cl}^-])[\text{S}_4\text{O}_6^{2-}][\text{HOCl}][\text{H}^+]$	$k_7 = (1.82 \pm 0.19) \times 10^7 \text{ M}^{-2} \text{ s}^{-1}$ $k'_7 = (2.35 \pm 0.58) \times 10^9 \text{ M}^{-3} \text{ s}^{-1}$ $\geq 10^7 \text{ M}^{-2} \text{ s}^{-1}$
R8	$k_8[\text{S}_2\text{O}_3\text{Cl}^-][\text{ClO}_2^-][\text{H}^+]$	$k_8/k_9 = 1.32 \pm 0.52$
R9	$k_9[\text{S}_2\text{O}_3\text{Cl}^-][\text{ClO}_2^-][\text{Cl}^-]$	
R10	$k_{10}[\text{HSO}_3^-][\text{ClO}_2^-][\text{H}^+]$	$(8.20 \pm 0.12) \times 10^9 \text{ M}^{-2} \text{ s}^{-1}$
R11	$k_{11}[\text{HSO}_3^-][\text{HOCl}]$	$7.6 \times 10^8 \text{ M}^{-1} \text{ s}^{-1}$ (ref 30)
R12	$k_{12}[\text{HOCl}][\text{S}_2\text{O}_3\text{ClO}_2^-][\text{Cl}^-]$	$(7.30 \pm 0.39) \times 10^7 \text{ M}^{-2} \text{ s}^{-1}$
R13	$k_{13}[\text{HOCl}][\text{S}_2\text{O}_3\text{ClO}_2^-][\text{Cl}^-][\text{OH}^-]$	$(3.36 \pm 0.28) \times 10^{16} \text{ M}^{-3} \text{ s}^{-1}$

^a No error indicates that the value was fixed during the fitting procedure.

agreement with the values found in the literature.^{12,20}

Steps R2 and R3 are the only reactions of $\text{S}_2\text{O}_3\text{OH}^-$ that need to be included for an adequate fit. The role of this species in the reaction of tetrathionate has been documented elsewhere.^{21,22} Both steps are fast, and their rate coefficients cannot be calculated individually; only their ratio can be determined. We therefore fixed $k_2 = 100 \text{ M}^{-1} \text{ s}^{-1}$ and determined k_3/k_2 . Since any value of k_2 higher than $10 \text{ M}^{-1} \text{ s}^{-1}$ leads to the same final result at fixed k_3/k_2 , we simply chose a reasonable, but arbitrary value for k_2 . The existence of the parallel steps R2 and R3 is supported by the following indirect evidence. First, eliminating either step not only increases significantly the average deviation, from 0.0041 to 0.0081 and 0.0070 absorbance unit for dropping R2 and R3, respectively, but also leads to systematic deviations between the measured and calculated values, especially at higher tetrathionate concentrations. As $[\text{S}_4\text{O}_6^{2-}]$ increases, the chlorine dioxide–tetrathionate reaction becomes more significant, and the $\text{S}_2\text{O}_3\text{ClO}_2^-$ formed in step R3 provides another link to the chlorine dioxide–tetrathionate subsystem in addition to chlorine dioxide itself. We attempted to replace step R2 with the plausible reaction



with no success. Several other efforts to eliminate either step R2 or R3 also failed, leading us to conclude that both of these reactions are required to quantitatively describe the formation of chlorine dioxide.

Step R4 is the well-known hypochlorous acid–chlorite reaction that has been studied by several authors,^{5,23–26} who give values of k_4 ranging from $1.06 \times 10^6 \text{ M}^{-2} \text{ s}^{-1}$ to $5.7 \times 10^6 \text{ M}^{-1} \text{ s}^{-1}$. The disagreement among these results likely stems from unrecognized general acid catalysis of this process. Since our experimental conditions were almost the same as those used in the study performed by Peintler et

(16) Horváth, D.; Tóth, Á. *J. Chem. Phys.* **1998**, *108*, 1447.

(17) Stier, D. E.; Boissonade, J. *Phys. Rev. E* **2004**, *70*, 016210.

(18) Boissonade, J.; Dulos, E.; Gauffre, F.; Kuperman, M. N.; De Kepper, P. *Faraday Discuss.* **2001**, *120*, 353.

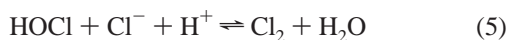
(19) Vasquez, D. A.; De Wit, A. *J. Chem. Phys.* **2004**, *121*, 935.

(20) Tóth, Á.; Horváth, D.; Siska, A. *J. Chem. Soc., Faraday Trans.* **1997**, *93*, 73.

(21) Kurin-Csörgei, K.; Orbán, M.; Rábai, G.; Epstein, I. R. *J. Chem. Soc., Faraday Trans.* **1996**, *92*, 2851.

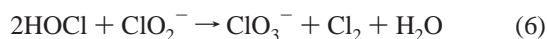
(22) Voslar, M.; Matejka, P.; Schreiber, I. *Inorg. Chem.* **2006**, *45*, 2824.

al.,⁵ we fixed the value of k_4 at their value, $1.06 \times 10^6 \text{ M}^{-1} \text{ s}^{-1}$. We also tried to fit this rate coefficient, but we encountered strong correlation among the parameters k_4 , k'_4 , k_5 , k_7 , k'_7 , k_{12} , and k_{13} . We therefore chose to use the value of k_4 found independently under the conditions that most closely correspond to our experiments. It should also be noted that the necessity of k'_4 in the fit suggests that the chloride ion has a significant impact on the kinetics of the hypochlorous acid–chlorite reaction. Nicoson and Margerum²⁷ found that chloride accelerates this reaction because of the well-known fast equilibrium²⁸



followed by the reaction between chlorine and the chlorite ion, which is much faster than the corresponding hypochlorous acid–chlorite reaction. They obtained a value of $5.7 \times 10^5 \text{ M}^{-1} \text{ s}^{-1}$ for the rate-determining step of the chlorite–chlorine reaction. Our calculated result, $k'_4 = (5.03 \pm 0.13) \times 10^8 \text{ M}^{-3} \text{ s}^{-1}$, gives a value of $3.1 \times 10^5 \text{ M}^{-1} \text{ s}^{-1}$ for the chlorite–chlorine reaction, in reasonable agreement with Nicoson's value,²⁷ if one uses the widely accepted equilibrium constant $K = 1640 \text{ M}^{-2}$ for eq 4 determined by Eigen and Kustin.²⁸ The agreement is even better if we use Nicoson's $K = 960 \text{ M}^{-2}$ for the chlorine hydrolysis, which yields $5.24 \times 10^5 \text{ M}^{-1} \text{ s}^{-1}$ for the rate coefficient of the chlorite–chlorine reaction.

Emmenegger and Gordon²⁴ suggested that step R5 accompanies the formation of chlorine dioxide in the reaction between hypochlorous acid and chlorite, giving chlorate in a separate pathway. Later this simple nucleophilic displacement was rejected by Peintler and co-workers⁵ because they found that the ratio of chlorine dioxide to chlorate formed decreases with pH. If step R5 is treated as a third-order process with rate proportional to $[\text{H}^+]$, this ratio would be independent of pH. The pH dependence of the $[\text{ClO}_2]/[\text{ClO}_3^-]$ ratio can be explained, however, if step R5 is a simple second-order process and step R4 is a third-order process whose rate is proportional to $[\text{H}^+]$. Instead of the simple nucleophilic displacement, Peintler et al. suggested the third-order process

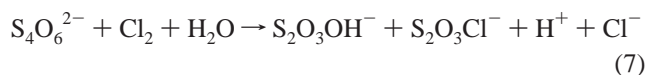


to explain their experimental findings. We tried to replace step R5 with reaction 6 with no success, probably because HOCl does not accumulate to a high enough level to allow this third-order process to dominate. The proposed role of R5 is also supported by the fact that its elimination from the kinetic model destroys the fit, resulting in a nearly 7-fold increase in the average deviation to 0.0282 absorbance units.

Step R6 is the well-known fast reaction that generates chlorine dioxide from Cl_2O_2 . In our previous work,¹⁰ we have

noted that the otherwise sluggish chloride ion catalyzes this reaction in another system. Here, we present further experimental evidence to support those findings. Our values of k_6 and k'_6 are in reasonable agreement with our previous determinations under very different experimental conditions.¹⁰

Step R7 is the initial step of the oxidation of tetrathionate by hypochlorous acid. A second-order rate coefficient, $32 \text{ M}^{-1} \text{ s}^{-1}$, was determined for this step in alkaline medium.⁷ Our previous considerations¹² and the experiments presented here suggest that the rate of this reaction must depend on the concentration of H^+ as well. This fact is hidden in the previously determined rate coefficient, since it was determined between pH 8.2 and 9.0, where the concentration of HOCl is roughly proportional to $[\text{H}^+]$, since the $\text{p}K$ of HOCl is 7.40.²⁹ We have found that this reaction is also catalyzed by the chloride ion, and this observation can easily be explained by the fast hydrolytic equilibrium of Cl_2 (eq 5) followed by



Steps R8 and R9 are fast reactions, whose individual values cannot be determined, since only their ratio affects the final fit. Our calculations reveal that k_8 has a lower limit of $10^7 \text{ M}^{-2} \text{ s}^{-1}$. Fixing k_8 at this value determines k_9 as $1.32 \times 10^7 \text{ M}^{-2} \text{ s}^{-1}$. These steps are crucial to the kinetic model. They imply that chloride not only increases the rate of consumption of chlorite by the intermediate $\text{S}_2\text{O}_3\text{Cl}^-$ but also alters the stoichiometry. All attempts to unify the stoichiometry by having parallel proton- and chloride-catalyzed paths were unsuccessful. Using the stoichiometry of step R8 with H^+ - and Cl^- -catalyzed pathways increased the average deviation to 0.0107 and introduced a systematic deviation between the measured and calculated curves, especially where the initial chloride concentration was varied. The stoichiometry of step R9 with both catalyzed pathways gave an acceptable average deviation of 0.0047, but at large chlorite excess, the simulated curves failed to reproduce the early phase of the kinetic curves in which the measured absorbance rises suddenly followed by a slower, nearly linear increase. These unsuccessful efforts were, however, helpful in understanding why both steps R8 and R9 are needed. At low chloride concentrations, step R8 converts $\text{S}_2\text{O}_3\text{Cl}^-$ and chlorite to HOCl, transforming all the chlorine atoms originating from the reactant chlorite into HOCl, which can ignite the HOCl-catalyzed path to produce chlorine dioxide sooner. If, however, the chloride concentration is sufficiently high, then step R8 is no longer needed, and $\text{S}_2\text{O}_3\text{Cl}^-$ and chlorite (in the presence of chloride) react according to step R9, in which only half of the converted chlorine produces HOCl (the rest is converted to chloride ion), preventing the autocatalytic buildup of HOCl.

Step R10 is the well-known oxidation of S(IV) by chlorite,

(23) Taube, H.; Dodgen, H. *J. Am. Chem. Soc.* **1949**, *71*, 3330.

(24) Emmenegger, F.; Gordon, G. *Inorg. Chem.* **1967**, *6*, 633.

(25) Aieta, E. M.; Roberts, P. X. *Environ. Sci. Technol.* **1986**, *20*, 50.

(26) Tang, T.-F.; Gordon, G. *Environ. Sci. Technol.* **1984**, *18*, 212.

(27) Nicoson, J. S.; Margerum, D. W. *Inorg. Chem.* **2002**, *41*, 342.

(28) Eigen, M.; Kustin, K. *J. Am. Chem. Soc.* **1962**, *84*, 1355.

(29) *IUPAC Stability Constant Database*; Royal Society of Chemistry: London, 1992–1997.

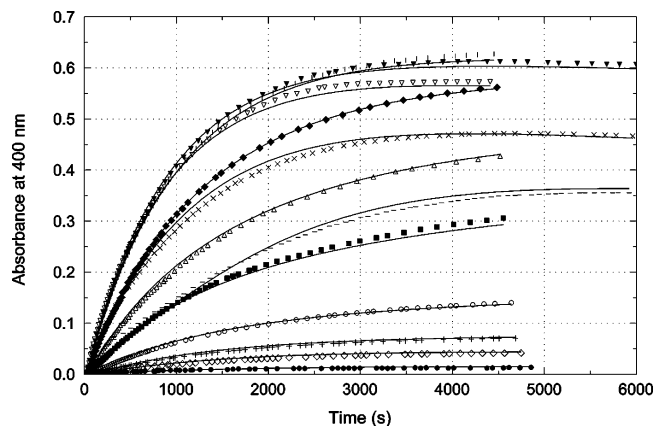


Figure 5. Measured (symbols) and calculated (solid lines) absorbances at pH = 4.65 and $[S_4O_6^{2-}]_0 = 0.5$ mM in the absence of chloride ion. $[ClO_2^-]_0$ (mM) = 0.5 (●), 1.4 (◇), 2.0 (+), 3.0 (○), 5.0 (■), 7.0 (△), 10.0 (◆), 14.0 (◻), 17.0 (▼), 20.0 (▽), 25.0 (×), and 30.0 (–).

which was studied previously by Huff Hartz,³¹ Frerichs,³² and their co-workers. Huff Hartz et al. conducted their experiments with a large excess of S(IV) to maintain pseudo-first-order conditions. Under their experimental conditions, which are very different from ours, where chlorite is always in huge excess over S(IV), k_{10} was found to be $5.01 \times 10^8 \text{ M}^{-2} \text{ s}^{-1}$, taking $pK_a(SO_2) = 1.90^{29}$ into account. Frerichs et al. obtained $2.19 \times 10^8 \text{ M}^{-2} \text{ s}^{-1}$ for k_{10} by simulating the oscillatory behavior of the chlorite–sulfite reaction in a continuously stirred tank reactor. We have obtained a somewhat higher value, $(8.20 \pm 0.12) \times 10^9 \text{ M}^{-2} \text{ s}^{-1}$, which agrees well with our earlier result.¹² Taking into account the uncertainty of $pK_a(SO_2)$, the long extrapolation from pH = 4.0 from which this value was determined,³¹ and the different experimental conditions, the 16-fold difference may be regarded as acceptable.

Step R11 is the fast oxidation of S(IV) by hypochlorous acid. The rate coefficient k_{11} was found³⁰ to be $7.6 \times 10^8 \text{ M}^{-1} \text{ s}^{-1}$, which is close to the diffusion-controlled limit. We fixed this parameter throughout the fitting procedure.

Steps R12 and R13 are the further reactions of $S_2O_3ClO_2^-$ with hypochlorous acid. These processes suggest that the reactive species ($Cl_2/HOCl/OCl^-$) can attack the proposed intermediate at two different sites, resulting in alternative products. Attempts to replace these reactions with other steps met with no success. Eliminating either of them increased the average deviation from 0.0041 to 0.0111 and 0.0112 for k_{12} and k_{13} , respectively, and also altered the experimentally measured trends in the presence of chloride ion.

Table 2 summarizes the fixed and fitted rate coefficients in the fitting procedure. Figures 5–9 demonstrate that the kinetic model presented here gives a good description of the formation of chlorine dioxide under our experimental conditions. The average deviation was 0.0041 for the absolute fit and 6.2% for the relative fit, which we believe to be close to the experimentally achievable limit of error.

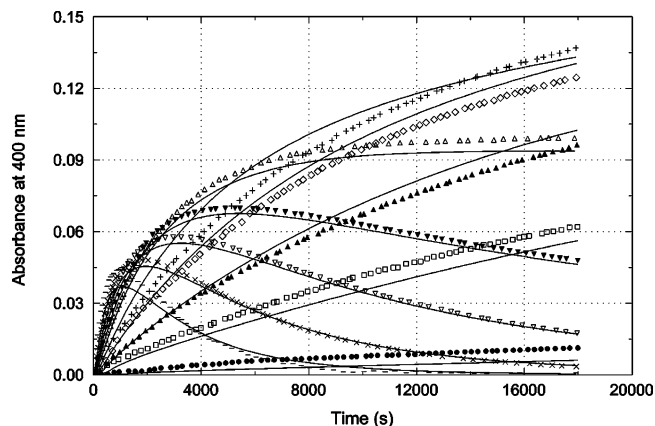


Figure 6. Measured (symbols) and calculated (solid lines) absorbances at pH = 5.07 and $[ClO_2^-]_0 = 5.0$ mM in the absence of chloride ion. $[S_4O_6^{2-}]_0$ (mM) = 0.1 (●), 0.14 (◻), 0.2 (▲), 0.3 (◇), 0.5 (+), 0.9 (△), 1.4 (▼), 2.0 (▽), 3.0 (×), and 5.0 (–).

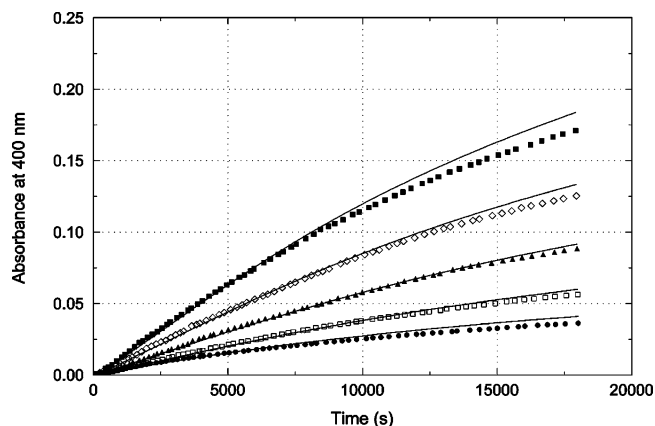


Figure 7. Chloride dependence of the measured (symbols) and calculated (solid lines) absorbances at pH = 5.35, $[ClO_2^-]_0 = 5.0$ mM, $[S_4O_6^{2-}]_0 = 0.3$ mM. $[Cl^-]_0$ (mM) = 0.0 (●), 1.0 (◻), 3.0 (▲), 6.0 (◇), and 10.0 (■).

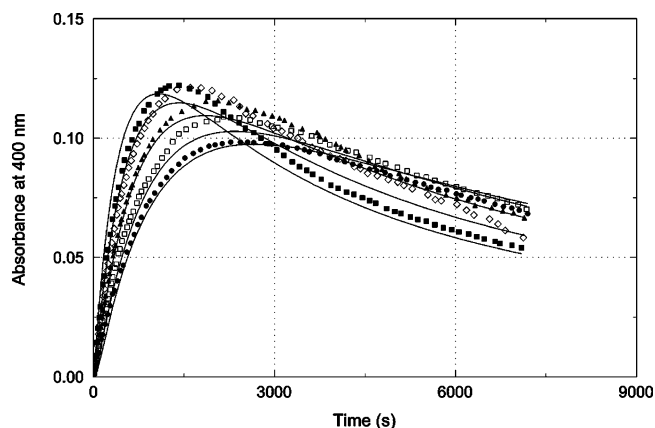


Figure 8. Chloride dependence of measured (symbols) and calculated (solid lines) absorbances at pH = 5.35, $[ClO_2^-]_0 = 5.0$ mM, $[S_4O_6^{2-}]_0 = 1.4$ mM. $[Cl^-]_0$ (mM) = 0.0 (●), 1.0 (◻), 3.0 (▲), 6.0 (◇), and 10.0 (■).

Finally, each of the three principal stoichiometries, eqs 1–3, is consistent with the proposed model. Equation 1 can be generated as $2*(R1) + 4*(R2) + (R10) + 7*(R11)$, a combination that assumes that hypochlorous acid never reacts with chlorite to yield either chlorine dioxide or chlorate. Equation 2 is obtained by combining $(R1) + 2*(R2) + 7*(R4) + 7*(R6) + 4*(R10)$, which produces no chlorate from the hypochlorous acid–chlorite reaction. Similarly, eq 3

(30) Fogelman, K. D.; Walker, D. M.; Margerum, D. W. *Inorg. Chem.* **1988**, *27*, 1672.

(31) Huff Hartz, K. E.; Nicoson, J. S.; Wang, L.; Margerum, D. W. *Inorg. Chem.* **2003**, *42*, 78.

(32) Frerichs, G. A.; Mlnarik, T. M.; Grun, R. J.; Thompson, R. C. *J. Phys. Chem. A* **2001**, *105*, 929.

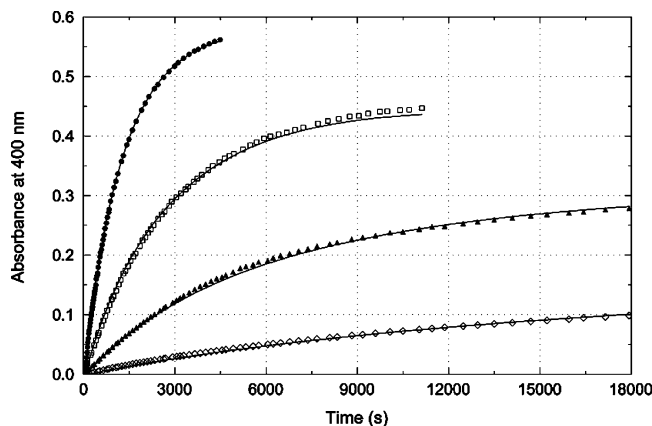


Figure 9. pH dependence of measured (symbols) and calculated (solid lines) absorbances in the initial absence of chloride ion at $[\text{ClO}_2^-]_0 = 10.0$ mM, $[\text{S}_4\text{O}_6^{2-}]_0 = 0.5$ mM. pH = 4.65 (●), 4.85 (□), 5.07 (▲), and 5.35 (◇).

comes about from $(\text{R1}) + 2*(\text{R2}) + 7*(\text{R5}) + 4*(\text{R10})$, yielding no chlorine dioxide formation. As we have seen, it is impossible to conform rigorously with any of these restrictions experimentally, and it is therefore clear that eqs 1–3 can only be regarded as theoretical limiting stoichiometries.

Conclusions

This study represents the first attempt to construct a kinetic model for the chlorite–tetrathionate reaction applicable over a wide range of initial reactant concentrations and in the presence and absence of the autocatalyst chloride ion over the entire time scale of the reaction. We demonstrated earlier¹¹ that the reaction proceeds via two parallel pathways: a direct reaction and a HOCl-catalyzed reaction. The five step-model suggested there for interpreting the unusual formal kinetic orders of the reactants is extended in this paper to explain the formation of chlorine dioxide on a longer time scale. We have also found that the chloride ion catalyzes the formation of chlorine dioxide, but this catalysis arises

from the chloride dependence of the hypochlorous acid–chlorite and hypochlorous acid–tetrathionate subsystems rather than from chloride catalysis of the direct reaction. The measured kinetic curves support our assertion that the slow direct reaction is not the only rate-determining step and confirm the essential role of the HOCl-catalyzed pathway. Although the chloride catalysis in the experiments presented here is relatively subtle (the formal kinetic order of chloride is around 0.3), together with the HOCl-catalysis, it may play a governing role in the spatiotemporal structures found recently^{16–20} in the chlorite–tetrathionate system.

We hope that the results presented here will inspire theoretical investigations of the proposed intermediates $\text{S}_2\text{O}_3\text{OH}^-$ and $\text{S}_2\text{O}_3\text{ClO}_2^-$, which could test our assumption of the parallel pairs of steps R2 and R3, as well as R8 and R9.

Finally we note that we have adopted without modification the previously proposed kinetic model of the chlorine dioxide–tetrathionate reaction. This was possible because the kinetic parameters of the CDT reaction were determined over wide concentration ranges of the reactants by simultaneous fitting of all measured kinetic curves without restriction to pseudo-first-order conditions. We believe strongly that complex reactions are best studied in this fashion, using data acquired over a broad set of conditions and building on studies of component subsystems.

Acknowledgment. This work was supported by the Hungarian Research Fund (Grant T047031) and the National Science Foundation (CHE-0306262 and CHE-0615507). A.K.H is grateful for the financial support of a Békesy György (B12/2003) postdoctoral fellowship.

Supporting Information Available: Files containing the measured and calculated absorbances for all the 152 kinetic curves. This material is available free of charge via the Internet at <http://pubs.acs.org>.

IC061332T